

Deep Adversarial Inconsistent Cognitive Sampling for Multi-view Progressive Subspace Clustering

Renhao Sun

Abstract—Deep multi-view clustering methods have achieved remarkable performance. However, all of them failed to consider the difficulty labels (uncertainty of ground-truth for training samples) over multi-view samples, which may result into a non-ideal clustering network for getting stuck into poor local optima during training process; worse still, the difficulty labels from multi-view samples are always inconsistent, such fact makes it even more challenging to handle. In this paper, we propose a novel Deep Adversarial Inconsistent Cognitive Sampling (DAICS) method for multi-view progressive subspace clustering. A multi-view binary classification (easy or difficult) loss and a feature similarity loss are proposed to jointly learn a binary classifier and a deep consistent feature embedding network, throughout an adversarial minimax game over difficulty labels of multi-view consistent samples. We develop a multi-view cognitive sampling strategy to select the input samples from easy to difficult for multi-view clustering network training. However, the distributions of easy and difficult samples are mixed together, hence not trivial to achieve the goal. To resolve it, we define a sampling probability with theoretical guarantee. Based on that, a golden section mechanism is further designed to generate a sample set boundary to progressively select the samples with varied difficulty labels via a gate unit, which is utilized to jointly learn a multi-view common progressive subspace and clustering network for more efficient clustering. Experimental results on four real-world datasets demonstrate the superiority of DAICS over the state-of-the-art methods.

Index Terms—Adversarial Inconsistent Samples, Cognitive Sampling, Multi-view Progressive Subspace Clustering, Generative Adversarial Networks.

I. INTRODUCTION

CLUSTERING is fundamental to computer vision and machine learning communities. With the emerging of big data, multi-view data clustering is vital to big data analytics, which aims to cluster the data into different groups by exploiting the complementary information from multiple feature spaces, with each of them corresponded to an individual view. To achieve nonlinear feature modeling, a number of Deep Neural Networks (DNN) based clustering methods [1], [2], [3], [4], [5], [6], [7], [8] have achieved the desirable results in single-view scenario. To further enhance the performance, substantial deep multi-view clustering methods [9], [10], [11], [12], [13], [14], [15], [16] are motivated.

Specifically, DCCA [9] proposed a deep extension of the linear canonical correlation analysis (CCA) to learn deep feature for multi-view clustering. MvDMF [14] presented a deep multi-view clustering method through graph regularized semi-nonnegative matrix factorization, to capture the hidden information of each view while learning a common latent space to facilitate clustering. MvSCN [10] performed deep multi-view spectral clustering, to project data objects from each view into a common space via deep neural network to

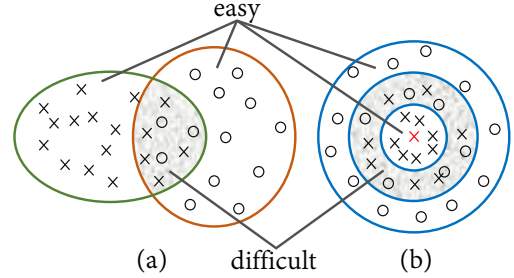


Fig. 1: (a) Samples \times and \circ in the shadow area \blacksquare that cannot be easily distinguished between two classes (\circ and \times denote class 1 and class 2, respectively) are difficult, and ones in the other area that can be categorized are easy. (b) According to (a), we know that, once the anchor \times is fixed, samples that are close (belong to the same class) and far (belong to a different class) from it are easy, and those within its middle (belong to unknown classes) in the shadow area \blacksquare are difficult.

preserve the local manifold invariance, meanwhile achieving the consistency of pairwise view-specific representation via Siamese Network [17]. Benefiting from adversarial learning [18], DAMC [13] pre-trained multi-view auto-encoder, and then jointly optimized auto-encoder and adversarial network to learn a common embedding for clustering. EAMC [16] jointly conducted adversarial learning and attention mechanism, where they are leveraged to align the latent feature distributions and quantify the importance of each view.

Despite the above progress, all of them ignore the difficulty labels (easy or difficult, see Fig. 1) of the training samples, *i.e.*, uncertainty of the ground-truth for training samples, for clustering network training, which will affect the performance and generalization of the training network. It is apparent that the network will overfit for all easy training samples, and poorly trained with all training samples to be difficult. Numerous strategies have been proposed to address the above problem of the single-view clustering, such as self-paced learning [19] and cognitive learning [4] strategies. However, it is not incrementally challenging for *deep* multi-view clustering, due to 1) the difficulty labels from multi-view samples are always inconsistent; 2) how to collaborate within deep multi-view spaces for training sampling as per difficulty label is challenging and rarely solved.

To solve the above problem, we propose a novel Deep Adversarial Inconsistent Cognitive Sampling (DAICS) method for multi-view progressive subspace clustering (see Fig. 2), where the flowchart mainly comprises three components: the **Adversarial Inconsistent Samples (AIS)** module, the **Cognitive Sampling (CS)** strategy and the multi-view clustering

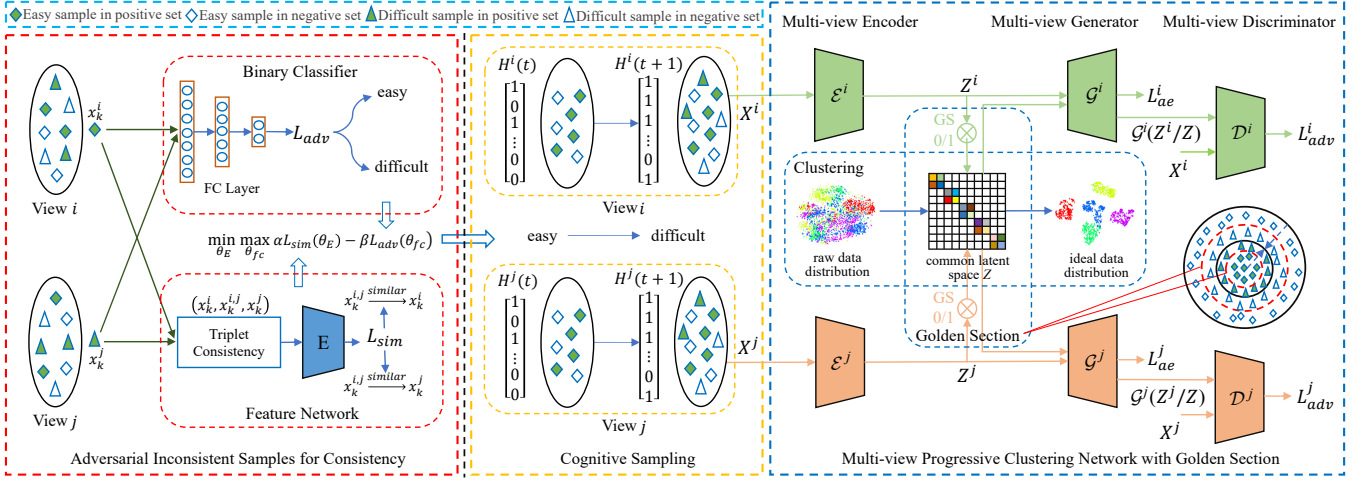


Fig. 2: The framework of DAICS (take the i -th and j -th views as example). DAICS consists of three components: the **Adversarial Inconsistent Samples (AIS) module**, **Cognitive Sampling (CS) strategy** and **Multi-view Progressive Clustering Network with Golden Section (GS) mechanism**. The goal of the AIS is to address the inconsistent difficulty labels of the multi-view samples via an adversarial minimax game of binary classifier and feature network. The CS strategy is proposed to gradually train the multi-view clustering network from easy to difficult samples. The GS is developed with two states via a gate unit (0 or 1) to train multi-view clustering network including encoder, generator and discriminator, while learning a common progressive subspace. The details are shown in Fig. 3, for subspace clustering.

network with the **Golden Section (GS)** mechanism. The basic idea of AIS is to convert samples with inconsistent difficulty labels into consistency by embedding samples from multiple views into a latent space via an adversarial minimax game between binary classifier and feature network. The binary classifier serves to *distinguish* the difficulty labels of multi-view inconsistent samples to train the deep consistent feature embedding network, and the feature network learns a common feature representation from the multi-view inconsistent samples to *confuse* the binary classifier. The multi-view CS strategy is developed to select the samples from easy to difficult according to the probability of the samples for the clustering network training. As indicated by [19], selecting from the easy-to-difficult sampling strategy could avoid getting stuck in poor local minima while capturing the intrinsic patterns of multi-view samples. For the network efficiency, the GS mechanism is designed with two states via a gate unit. One is to learn the latent representation and the clustering network of each view relying on easy samples. The other learns a multi-view common progressive subspace to coordinate all views with both easy and difficult samples, where the samples are progressively processed, leading to a multi-view progressive subspace clustering.

The major technical contributions are summarized below:

- A novel DAICS method is proposed to consider the difficulty labels of the samples for deep multi-view subspace clustering.
- A multi-view cognitive sampling strategy is developed to select samples from easy to difficult with getting stuck in poor local minima being avoided.
- To achieve the clustering network training efficiency, we present a golden section mechanism

to learn a multi-view common progressive subspace via a gate unit (0 or 1).

The extensive ablation studies validate the advantages of DAICS.

II. RELATED WORKS

A. Subspace clustering

To date, massive subspace clustering algorithms [20], [21], [22], [23], [24], [25], [26], [27] have been proposed, among them, spectral subspace clustering is one of the popular linear algorithms to cluster high-dimensional data [24]. The most challenging problem in spectral subspace clustering is the construction of affinity matrix. Existing studies on affinity matrix in spectral subspace clustering could be classified into three main groups: 1) matrix factorization based algorithms [26], [27], 2) model based algorithms [21], 3) self-expression based algorithms [28], [29]. These algorithms perform spectral subspace clustering on the affinity matrix to cluster the high-dimensional data points. Nevertheless, the processing of high-dimensional data always takes expensive time and computation. The sparse subspace clustering algorithms [20], [22], [23] have been developed to infer the clustering of data points into a low-dimensional subspace by solving a sparse optimization program whose solution is used in spectral subspace clustering algorithms. However, these algorithms are not able to model the non-linear and high-dimensional complex real-world data because of they can only cluster linear subspace. To resolve it, the deep subspace clustering algorithms have been proposed and attracted plenty of attention, which will be detailed in the next section.

B. Deep Clustering

Inspired by deep learning [30], [31], the deep clustering algorithms have been developed to model the non-linear and high-dimensional complex data, and have enough capacity to deal with the large-scale datasets. There are two main branches of the existing methods. One branch is based on the auto-encoder networks, which is aiming to learn a common latent representation by reconstructing the input samples for a better clustering. Ji *et al.* [6] proposed an unsupervised subspace clustering method that was built upon deep auto-encoders, and introduced a self-expressive layer to learn pairwise affinities for clustering. Based on the above, Zhang *et al.* [7] presented a neural collaborative subspace clustering algorithm to construct negative and positive two confidence affinity matrices, which could supervise each other to promote training. Yang *et al.* [2] and Zhang *et al.* [8] developed a self-supervised module that exploited the output of spectral clustering [32] to achieve optimal clustering results. For the model robustness, Jiang *et al.* [33] contributed a duet robust deep subspace clustering, to handle contaminated data and enhance the robustness from both the self-expressive and the data reconstruction perspective with two regularization norms. In addition, a robust deep subspace clustering framework [4] was proposed, based on the principle of human cognitive process, learning gradually samples from easy to difficult and less to more.

The other is based on the joint deep learning framework of the auto-encoders and the Generative Adversarial Networks (GANs) [18], compared to the previous branch, a discriminator network is introduced to further capture the data distribution and disentangle the common latent representation for a better clustering. In the single-view clustering methods, a Cluster-GAN [34] is proposed as a new mechanism using GANs by sampling latent variables for clustering, to preserve latent representation interpolation across categories for clustering. Almost contemporaneously, due to deep models with large number of parameters prone to overfitting, Dizaji *et al.* [19] presented a deep generative adversarial clustering network with a balanced self-paced learning algorithm to tackle the problem. In the multi-view clustering methods, Li *et al.* [13] developed a deep adversarial multi-view clustering (DAMC) network to learn the intrinsic structure of multi-view samples, which consists of a deep auto-encoder and an adversarial learning process for each view, for a better clustering. However, the more complex the models are, the larger the number of parameters are. The deep models prone to the overfitting leading to get stuck in poor local minima for multi-view clustering. Therefore, starting from the difficulty labels of the multi-view samples, we propose a deep adversarial inconsistent cognitive sampling (DAICS) method to efficiently train deeper networks for multi-view progressive subspace clustering.

C. Self-paced Learning Algorithms

Self-paced learning derives from curriculum learning [35], a human-like learning principle where the easier instances are learned first, and then more difficult instances are gradually introduced to the learning process. Kumar *et al.* [36] proposed a self-paced learning algorithm to learn a new parameter

vector from easy samples to difficult samples, compared to curriculum learning, the self-paced learning automatically adjusted the sample difficulty. Jiang *et al.* [37] developed an extension of the self-paced learning algorithm, the diversity is introduced to a general regularization term. Many works [38], [39], [40] further considered self-paced learning into various tasks to avoid getting stuck in poor local minima and improve the generalization for models. For the clustering tasks, the self-paced learning was used to the single-view clustering to improve the robustness of the models. Unlike the single-view clustering, multi-view clustering relies on the complementary information from the samples of multiple views. The application of cognitive learning on the multi-view clustering is not a simple extension from one on the single-view clustering. The process of which is demanded to collaborate with the difficulty labels (easy or difficult) of multi-view samples.

III. THE PROPOSED METHOD

In this section, our proposed DAICS method is illustrated in Fig. 2, which clusters a set of n data objects with V views $D = \{\mathbf{X}^1, \dots, \mathbf{X}^i, \dots, \mathbf{X}^V\}$ into c clusters, where $\mathbf{X}^i \in \mathbb{R}^{d_i \times n}$ denotes the samples of the dimension d_i from the i -th view. The DAICS that consists of three components: the adversarial inconsistent samples (AIS) module, the cognitive sampling (CS) strategy and the multi-view clustering network with the golden section (GS) mechanism will be elaborated in detailed, together with their implementation.

A. Adversarial Inconsistent Samples

Given $\mathbf{X}^i = \{x_1^i, \dots, x_n^i\}$ of the i -th view. Following [41], as shown in Fig. 3(a), we obtain the positive sample set \mathbf{P}^i , w.r.t. $\mathbf{R}_{\mathbf{P}^i}$ and the negative sample set \mathbf{N}^i w.r.t. $\mathbf{R}_{\mathbf{N}^i}$ by K Nearest Neighbors (K-NN) algorithm. For \mathbf{P}^i and \mathbf{N}^i , we further determine the difficulty label of x_k^i by the distance from a randomly selected anchor object such as x_a^i , resulting into the distributions of samples from easy to difficult for $\mathbf{R}_{\mathbf{P}^i}$ and $\mathbf{R}_{\mathbf{N}^i}$. For \mathbf{P}^i , if the distance to x_a^i is small, it is more likely to be easy, *i.e.*, certain to be the same group as x_a^i , while for \mathbf{N}^i , the large distance to x_a^i is more likely to be easy, *i.e.*, certain to be the different group from x_a^i . To this end, the difficulty label of x_k^i is defined as

$$y_k^i = \begin{cases} 0, & d_k^{\mathbf{N}^i} > \mu d_{max}^{\mathbf{N}^i} \text{ or } d_k^{\mathbf{P}^i} < \mu d_{max}^{\mathbf{P}^i} \\ 1, & \text{otherwise} \end{cases}, \quad (1)$$

where $y_k^i = 0$ (1) indicates that the label of sample x_k^i is easy (difficult). $d_k^{\mathbf{N}^i}$ and $d_k^{\mathbf{P}^i}$ denote the distance between x_k^i and x_a^i in the set \mathbf{N}^i and \mathbf{P}^i , respectively. $d_{max}^{\mathbf{N}^i}$ and $d_{max}^{\mathbf{P}^i}$ denote the maximum distance from the anchor x_a^i in \mathbf{N}^i and \mathbf{P}^i , respectively. μ is a boundary factor for easy and difficult samples.

As it is widely known, the difficulty labels of multi-view samples are always inconsistent. We develop an adversarial strategy to make the difficulty labels of such pairs of samples to be consistent. Our model comprises a binary classifier that

generates the difficulty labels of the fused sample representations throughout a fully connected network, equipped with an adversarial cross-entropy loss to yield a pseudo difficulty label. Another feature embedding network is learned to achieve a common representation for inconsistent samples. The difficulty labels are obtained via a hinge loss. Afterwards, such two labels are processed throughout an adversarial minimax game to yield the consistent difficulty labels. In what follows, we discuss the details for the binary classifier and the feature embedding network.

1) *Binary Classifier*: After determining the difficulty labels of all samples via Eq. (1), it is trivial to collect the samples with inconsistent labels. Assume any pair of inconsistent samples (x_k^i, x_k^j) , such that $y_k^i \neq y_k^j$.

We propose a binary classifier to minimize the binary classification throughout an adversarial loss, as formulated below:

$$\mathcal{L}_{adv}(\theta_{fc}) = -\frac{1}{K} \sum_{y_k^i \neq y_k^j} \ell(\log f(x_k^i) + \log(1 - f(x_k^j))), \quad (2)$$

where \mathcal{L}_{adv} denotes the cross-entropy loss to classify all K pairs of samples with inconsistent difficulty labels into the binary value (0/1) for easy or difficult. ℓ is a factor of the pseudo difficulty label, such that $0 \leq \ell \leq 1$. $f(\cdot)$ is a binary classifier including three fully connected layers with the parameters θ_{fc} , with its output to be 0 or 1, which is generated to guide the training process of the deep consistent embedding feature network that is discussed in the next.

2) *Feature Network*: Based on the pair $\{x_k^i, x_k^j\}$, we construct a triplet $\{x_k^i, x_k^{i,j}, x_k^j\}$, as the dimension for all three samples are distinct, we expect that $x_k^{i,j}$ is similar to both x_k^i and x_k^j within the output space of the feature network. Motivated by this, we define a deep feature embedding network \mathbf{E} , formulated as

$$\Delta x_k^{i,j} = \arg \min_{x_k^{i,j}} \left\| F(x_k^{i,j}) - F(x_k^j) \right\|_2^2, \quad (3)$$

s.t.

$$\left\| F(x_k^{i,j}) - F(x_k^i) \right\|_\infty < \xi,$$

where $F(\cdot)$ denotes the output for \mathbf{E} parameterized as θ_E . ξ denotes a factor. According to Eq. (3), the following constraint is satisfied:

$$\left\| F(x_k^{i,j}) - F(x_k^i) \right\|_2^2 > \left\| F(x_k^{i,j}) - F(x_k^j) \right\|_2^2. \quad (4)$$

However, the common feature representation extracted from the sample $x_k^{i,j}$ is not only similar to that of x_k^i but also similar to that of x_k^j . Hence, we aim at the following:

$$\left\| F(x_k^{i,j}) - F(x_k^i) \right\|_2^2 < \left\| F(x_k^{i,j}) - F(x_k^j) \right\|_2^2. \quad (5)$$

Eq. (4) and Eq. (5) all together comprise an adversarial learning process, to facilitate mutual learning over easy and

Algorithm 1 Pseudocode of optimizing our AIS

Initialization: k samples of the i -th view: $\{x_1^i, \dots, x_k^i\}$;
 k samples of the j -th view: $\{x_1^j, \dots, x_k^j\}$;
Hyperparameters: $t, m, \ell, \alpha, \beta$;
Batch size: b ;
Update until convergence:
1: **for** t steps **do**
2: Update the parameters θ_E of the embedding feature network by descending their stochastic gradients:
3: $\theta_E \leftarrow \theta_E - \eta \cdot \nabla_{\theta_E} \frac{1}{b} (\alpha \mathcal{L}_{sim} - \beta \mathcal{L}_{adv})$
4: **end for**
5: Update the parameters θ_E of the binary classifier by ascending their stochastic gradients:
6: $\theta_{fc} \leftarrow \theta_{fc} + \eta \cdot \nabla_{\theta_{fc}} \frac{1}{b} (\alpha \mathcal{L}_{sim} - \beta \mathcal{L}_{adv})$
7: **return** Learned embedding feature $F(\cdot)$ and binary classifier $f(\cdot)$

difficult samples. Based on that, the feature similarity loss is defined as follows:

$$\mathcal{L}_{sim}(\theta_E) = \frac{1}{K} \sum_{y_k^i \neq y_k^j} \max(0, m + \left\| F(x_k^{i,j}) - F(x_k^i) \right\|_2^2 - \left\| F(x_k^{i,j}) - F(x_k^j) \right\|_2^2), \quad (6)$$

where \mathcal{L}_{sim} denotes a hinge loss [42], [43]. m is the margin, indicating a similarity preference factor. When m is a smaller value, the network can obtain the better performance.

3) *Adversarial Learning*: The final consistent difficulty labels for (x_k^i, x_k^j) are obtained via the adversarial learning process of the binary classification loss \mathcal{L}_{adv} and the feature similarity loss \mathcal{L}_{sim} , to jointly learn the binary classifier $f(\cdot)$ and the feature network $F(\cdot)$, formulated as a **minimax game** with the following objectives:

$$\hat{\theta}_E = \arg \min_{\theta_E} (\alpha \mathcal{L}_{sim}(\theta_E) - \beta \mathcal{L}_{adv}(\hat{\theta}_{fc})), \quad (7)$$

$$\hat{\theta}_{fc} = \arg \max_{\theta_{fc}} (\alpha \mathcal{L}_{sim}(\hat{\theta}_E) - \beta \mathcal{L}_{adv}(\theta_{fc})). \quad (8)$$

We summarize the above process in Algorithm 1.

B. Cognitive Sampling

Upon the consistent difficulty labels of the training multi-view samples, we aim at selecting from easy to difficult, to avoid trapping in poor local minima resulting into undesirable generalization. However, as illustrated in Fig. 3(a), the distributions of easy and difficult samples are mixed together, and hence not trivial to solve. To this end, we define a sampling probability, such that the probability of easy sample is larger than difficult one.

For both easy and difficult samples, we consider them in both positive and negative sets. Specifically, if the label of the sample x_k^i is easy, the probability p_{ke}^i is defined as follows:

$$p_{ke}^i = \begin{cases} \frac{d_{ke}^i}{d_{\max}^i}, & x_k^i \in \mathbf{N}^i \\ 1 - \frac{d_{ke}^i}{d_{\max}^i}, & x_k^i \in \mathbf{P}^i \end{cases}, \quad (9)$$

where d_{ke}^i denotes the distance between x_k^i and the anchor x_a^i . d_{\max}^i denotes the maximum distance between $x_k^i \in \mathbf{N}^i$ and x_a^i . According to Eq. (9), for $x_k^i \in \mathbf{N}^i$, the larger distance to x_a^i , the larger probability to be sampled (more easily determined to be a different group as x_a^i). For $x_k^i \in \mathbf{P}^i$, the smaller distance to x_a^i , the larger probability to be sampled (more easily determined to be the same group as x_a^i).

If the label of the sample x_k^i is difficult, we define the following:

$$p_{kd}^i = \frac{|d_{kd}^i - d_{med}^i|}{\sum_{l=1}^{n_d} d_l^i}, \quad (10)$$

where d_{kd}^i denotes the distance between x_k^i and x_a^i . d_{med}^i denotes the median distance among the distances of all n_d difficult samples to x_a^i . It is easily seen from Eq. (10) that the smaller distance between x_k^i and easy samples in both positive and negative sets, the larger p_{kd}^i is, otherwise, the smaller it is. The last question is whether $p_{ke}^i > p_{kd}^i$ to ensure the sequence from easy to difficult, which is answered in the following theorem.

Theorem 1: $p_{ke}^i > p_{kd}^i$

Proof 1: Empirically, $n_d \gg 1$ to ensure $\sum_{l=1}^{n_d} d_l^i > d_{\max}^i$, hence we consider the numerator of Eqs. (9) and (10). If x_k^i is easy and $x_k^i \in \mathbf{N}^i$, as shown in Fig. 3(a), it is obvious that, for any difficult sample, we have $0 < d_{kd}^i < d_{ke}^i$, $0 < d_{med}^i < d_{ke}^i$, hence it yields $|d_{kd}^i - d_{med}^i| < d_{ke}^i$. If $x_k^i \in \mathbf{P}^i$, the numerator of p_{ke}^i is $d_{\max}^i - d_{ke}^i$, it is apparent that $0 < d_{kd}^i < d_{\max}^i$, $0 < d_{med}^i < d_{\max}^i$. Meanwhile $0 < d_{ke}^i < d_{kd}^i$, $0 < d_{ke}^i < d_{med}^i$. Hence, we have $|d_{kd}^i - d_{med}^i| < d_{\max}^i - d_{ke}^i$. It finally leads to $p_{kd}^i < p_{ke}^i$. ■

For V views, we define $\mathbf{H}^i(t) = \{h_1^i(t), \dots, h_n^i(t)\}$ with $h_k^i(t)$ as a binary-value (0/1) to decide whether x_k^i is selected. To ensure the selection the samples from easy to difficult among V views, $h_k^i(t)$ is defined by

$$h_k^i(t) = \begin{cases} 1, & \lambda(t) \leq \frac{1}{V} \sum_{i=1}^V p_k^i \\ 0, & \text{otherwise} \end{cases}, \quad (11)$$

where $\lambda(t) \in [0, 1]$ is a self-adjusting sampling pace. p_k^i is the sampling probability of x_k^i as per Eqs. (9) and (10). For each view, e.g., the i -th view, we average the sampling probability for all V views. When the training process started, $\lambda(t)$ is a higher value so that only easy samples are selected. With the iteration number t increases, $\lambda(t)$ is decreasing to select difficult samples. Specifically, the difficult samples closer to easy samples are selected first, followed by others. Next, we discuss how to train the multi-view clustering network and learn a common progressive subspace via the easy and difficult samples.

C. Multi-view Progressive Clustering Network with Golden Section

Our multi-view clustering network adopts the architecture of auto-encoder combined with GAN [44], [13], which consists of multi-view encoder network, multi-view generator network and multi-view discriminator network for each view.

Multi-view encoder network \mathcal{E}^i : Our multi-view encoder networks are different for the diverse feature dimensions of

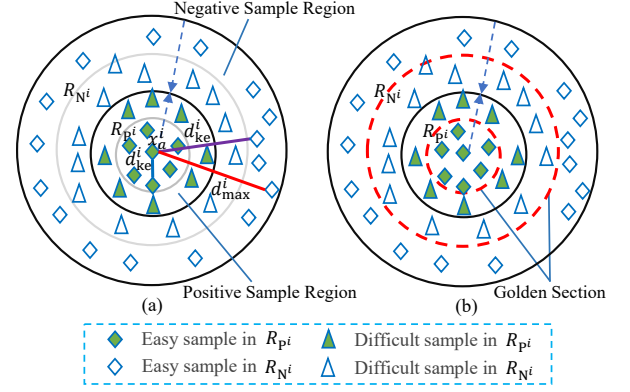


Fig. 3: For the i -th view, (a): R_{Pi} and R_{Ni} denote the positive and negative sample region. The difficulty labels of multi-view samples are defined via Eq. (1) and the samples from easy to difficult are gradually selected via Eqs. (9), (10) and (11). (b): The red slash circles in R_{Pi} and R_{Ni} denote the golden section to divide multi-view clustering network to two states via a gate unit to learn a common progressive subspace (see Eq. (12) for the details).

each view, there are multi-layer convolution neural networks with distinctive parameters. For the i -th view, given $\mathbf{X}^i = \{x_1^i, \dots, x_n^i\}$, the multi-view encoder \mathcal{E}^i aims to learn the latent representations $\mathbf{Z}^i = \{z_1^i, \dots, z_n^i\}$. Specifically, it maps the d_i -dimensional input sample x^i to a low-dimensional latent representation z^i . This mapping could be represented as $\mathbf{Z}^i = E_i(\mathbf{X}^i; \Theta_{\mathcal{E}^i})$, where $E_i(\cdot)$ refers to the i -th view's encoder network parameterized by $\Theta_{\mathcal{E}^i}$.

Multi-view generator network \mathcal{G}^i : Our multi-view generator network \mathcal{G}^i is set as a symmetrical architecture of multi-view encoder network \mathcal{E}^i for the i -th view, which consists of opposite multi-layer convolution neural networks with distinctive parameters. Specifically, the network \mathcal{G}^i can generate the reconstructed samples $\hat{\mathbf{X}}^i$ with the latent representations $\mathbf{Z}^i = \{z_1^i, \dots, z_n^i\}$ corresponding to the i -th view. We suppose $\hat{\mathbf{X}}^i = G_i(\mathbf{Z}^i; \Theta_{\mathcal{G}^i})$, where $G_i(\cdot)$ refers to the i -th view's generator network parameterized by $\Theta_{\mathcal{G}^i}$.

Multi-view discriminator network \mathcal{D}^i : Our multi-view discriminator network \mathcal{D}^i consists of 3 fully connected layers, which can distinguish a generated sample or a real sample. $\mathcal{D}^i(\cdot)$ parameterized by $\Theta_{\mathcal{D}^i}$ feeds back the result to generator network and updates the parameters of generator. By this means, the discriminator \mathcal{D}^i works as a regularizer to guide the training of our multi-view encoder network \mathcal{E}^i , which enhances the robustness of embedding representations and avoids the overfitting issue effectively.

Our goal is to learn a multi-view common subspace for clustering, while conducting multi-view clustering network collaboration throughout the common subspace. One natural question is about the training set for the multi-view common subspace learning and the clustering network learning. First, the overfitting will occur for the common subspace learning with easy training samples only, hence we proposed to learn that once handling difficult training samples. Second, to avoid trapping into poor local optima for clustering network, the easy

samples are ideal for initial training, then the difficult ones are gradually joining into the training process for an effective multi-view progressive clustering network.

1) *Golden Section*: We design a golden section (GS) mechanism, which detects whether the number of the training samples reach the golden section via a gate unit, seen as the two red slash circles in Fig. 3(b). According to Eq. (11), for the t -th iteration of the training process, the number of the input samples is calculated as $\sum_{k=1}^n h_k^i(t)$. Therefore, we have:

$$GS = \begin{cases} 1, & \sum_{k=1}^n h_k^i(t) > \sigma N^i \\ 0, & \text{otherwise} \end{cases}, \quad (12)$$

where N^i denotes the number of all samples for the i -th view. σ is a golden section factor, which is exactly the boundary factor μ in Eq. (1), the value is $(\sqrt{5}-1)/2 \approx 0.618$. Two states are yielded via a gate unit. $GS = 0$ (closed state) indicates that the number of the samples is below the golden section. The network only learns the corresponding latent representations of each view; $GS = 1$ (open state) indicates exceeding the golden section, where the multi-view common progressive subspace is learned upon multi-view latent representations and the different network modules from each view. The above two states result into the different loss functions for the multi-view clustering network to be optimized. We discuss each of them in the next.

2) *The Auto-Encoder Loss*: The auto-encoder loss is measured by L_2 distance between the reconstructed sample and the real sample, when $GS = 0$, the loss for the i -th view is

$$\hat{\mathcal{L}}_{ae}^i(\Theta_{\mathcal{E}^i}; \Theta_{\mathcal{G}^i}) = \|\mathbf{X}^i - \hat{\mathbf{X}}^i\|^2. \quad (13)$$

For $GS = 1$, the common subspace \mathbf{Z} depends on the latent representations of all views, meanwhile learned throughout the network training. Then, we have

$$\tilde{\mathcal{L}}_{ae}^i(\Theta_{\mathcal{E}^i}; \Theta_{\mathcal{G}^i}) = \|\mathbf{X}^i - \hat{\mathbf{X}}^i\|^2 + \lambda_i (\|\mathbf{X}^i - \tilde{\mathbf{X}}^i\|^2 + \|\mathbf{Z}^i - \mathbf{Z}\|^2), \quad (14)$$

where λ_i denotes a factor with the value $1/V$. $\tilde{\mathbf{X}}^i = G_i(\mathbf{Z}; \Theta_{\mathcal{G}^i})$ and $\mathbf{Z}^i = E_i(\mathbf{X}^i; \Theta_{\mathcal{E}^i})$. The reconstructed sample $\tilde{\mathbf{X}}^i = G_i(\mathbf{Z}; \Theta_{\mathcal{G}^i})$. We learn the common subspace \mathbf{Z} by minimizing the reconstruction loss with \mathbf{Z}^i , while confusing discriminator between \mathbf{X}^i and $\hat{\mathbf{X}}^i$ when $GS = 0$. Besides, \mathbf{X}^i and $\tilde{\mathbf{X}}^i$ is added when $GS = 1$, modeled by the following adversarial loss.

Minimizing the auto-encoder loss to optimize our multi-view auto-encoder networks aims to learn the bidirectional mapping between the raw sample space and the common subspace. However, for each view, the L_2 distance function focuses on each sample dimension separately while ignoring the correlations between sample dimensions, which maybe lead to blurred reconstructed results and cannot model the sample distribution of each view. In the next, we detail the adversarial loss in our model to alleviate this problem.

3) *The Adversarial Loss*: Following GAN [18], for the i -th view, it consists of a generator \mathcal{G}^i and a discriminator \mathcal{D}^i . When $GS = 0$, for the i -th view, we suppose that the sample

Algorithm 2 The proposed DAICS algorithm

Initialization: The dataset $\mathbf{D} = \{\mathbf{X}^1, \dots, \mathbf{X}^i, \dots, \mathbf{X}^V\}$;

Hyperparameters: $t, m, \ell, \alpha, \beta$;

Update until convergence:

- 1: Adopt the AIS algorithm (Algorithm 1) to obtain the samples with difficult consistency
 - 2: **for** t steps **do**
 - 3: Use the CS algorithm to gradually increase the sample from easy to difficult
 - 4: **if** $GS == 0$ **then**
 - 5: Update $\Theta_{\mathcal{E}^i}$ and $\Theta_{\mathcal{G}^i}$ via the Eq.13:
 $\Theta_{\mathcal{E}^i}, \Theta_{\mathcal{G}^i} \leftarrow \min \hat{\mathcal{L}}_{ae}^i(\Theta_{\mathcal{E}^i}; \Theta_{\mathcal{G}^i})$
 - 6: Update $\Theta_{\mathcal{D}^i}$ via the Eq.15:
 $\Theta_{\mathcal{D}^i} \leftarrow \max \mathbb{E}_{x^i \sim P(\mathbf{X}^i)} [\log D_i(x^i)] + \mathbb{E}_{\hat{x}^i \sim P(\hat{\mathbf{X}}^i)} [1 - \log D_i(\hat{x}^i)]$
 - 7: Update $\Theta_{\mathcal{E}^i}, \Theta_{\mathcal{G}^i}$ via the Eq.15:
 $\Theta_{\mathcal{G}^i} \leftarrow \min \mathbb{E}_{\hat{x}^i \sim P(\hat{\mathbf{X}}^i)} [1 - \log D_i(\hat{x}^i)]$
 - 8: **else**
 - 9: Update $\Theta_{\mathcal{E}^i}, \Theta_{\mathcal{G}^i}$ via the Eq.14:
 $\Theta_{\mathcal{E}^i}, \Theta_{\mathcal{G}^i} \leftarrow \min \tilde{\mathcal{L}}_{ae}^i(\Theta_{\mathcal{E}^i}; \Theta_{\mathcal{G}^i})$
 - 10: Update $\Theta_{\mathcal{D}^i}$ via the Eq.15:
 $\Theta_{\mathcal{D}^i} \leftarrow \max \mathbb{E}_{x^i \sim P(\mathbf{X}^i)} [\log D_i(x^i)] + \mathbb{E}_{\hat{x}^i \sim P(\hat{\mathbf{X}}^i)} [1 - \log D_i(\hat{x}^i)]$
 - 11: Update $\Theta_{\mathcal{E}^i}, \Theta_{\mathcal{G}^i}$ via the Eq.15:
 $\Theta_{\mathcal{G}^i} \leftarrow \min \mathbb{E}_{\hat{x}^i \sim P(\hat{\mathbf{X}}^i)} [1 - \log D_i(\hat{x}^i)]$
 - 12: Calculate the common subspace \mathbf{Z} by
 $\mathbf{Z} \leftarrow \frac{1}{V} \sum_{i=1}^V \mathbf{Z}^i$
 - 13: Update $\Theta_{\mathcal{D}^i}$ via the Eq.16:
 $\Theta_{\mathcal{D}^i} \leftarrow \max \mathbb{E}_{x^i \sim P(\mathbf{X}^i)} [\log D_i(x^i)] + \mathbb{E}_{\hat{x}^i \sim P(\hat{\mathbf{X}}^i)} [1 - \log D_i(\hat{x}^i)]$
 - 14: Update $\Theta_{\mathcal{E}^i}, \Theta_{\mathcal{G}^i}$ via the Eq.16:
 $\Theta_{\mathcal{G}^i} \leftarrow \min \mathbb{E}_{\hat{x}^i \sim P(\hat{\mathbf{X}}^i)} [1 - \log D_i(\hat{x}^i)]$
 - 15: **end if**
 - 16: Update the cluster centers \mathbf{U} and cluster indicator matrix \mathbf{S} via the Eq.17:
 $\mathbf{U}, \mathbf{S} \leftarrow \min \|\mathbf{Z} - \mathbf{US}\|_F^2$
 - 17: **end for**
 - 18: **return** Multi-view encoder $\Theta_{\mathcal{E}^i}$ and the cluster \mathbf{U}, \mathbf{S}
-

$x^i \sim P(\mathbf{X}^i)$, and the generated one is $\hat{x}^i \sim P(\hat{\mathbf{X}}^i)$. The adversarial loss is formulated as

$$\hat{\mathcal{L}}_{adv}^i(\Theta_{\mathcal{E}^i}; \Theta_{\mathcal{G}^i}; \Theta_{\mathcal{D}^i}) = \mathbb{E}_{x^i \sim P(\mathbf{X}^i)} [\log D_i(x^i)] + \mathbb{E}_{\hat{x}^i \sim P(\hat{\mathbf{X}}^i)} [1 - \log D_i(\hat{x}^i)], \quad (15)$$

where $D_i(\cdot)$ is required to distinguish \mathbf{X}^i and $\hat{\mathbf{X}}^i$. When $GS = 1$, the generated sample is $\tilde{x}^i \sim P(\tilde{\mathbf{X}}^i)$ obtained by the common subspace \mathbf{Z} , namely $\tilde{\mathbf{X}}^i = G_i(\mathbf{Z}; \Theta_{\mathcal{G}^i})$. That can be described as

$$\tilde{\mathcal{L}}_{adv}^i(\Theta_{\mathcal{E}^i}; \Theta_{\mathcal{G}^i}; \Theta_{\mathcal{D}^i}) = \mathbb{E}_{x^i \sim P(\mathbf{X}^i)} [\log D_i(x^i)] + \mathbb{E}_{\tilde{x}^i \sim P(\tilde{\mathbf{X}}^i)} [1 - \log D_i(\tilde{x}^i)]. \quad (16)$$

At the moment, in addition to the Eq. (15), $D_i(\cdot)$ is required to distinguish \mathbf{X}^i and $\tilde{\mathbf{X}}^i$. By training the multi-view encoder networks and the multi-view generator networks, we generate

fake sample similar to real sample of each view. The discriminators are trained to distinguish the fake sample from the real sample of each view. They play a min-max game until convergence. We can obtain a common subspace similar to the sample distribution of each view. According to the common subspace, we adopt a simple and effective k-means clustering algorithm to cluster different categories.

4) *The Clustering Loss*: Once multi-view common subspace $\mathbf{Z} = [z_1, \dots, z_n] \in \mathbb{R}^{p \times n}$ for n data objects with p dimensions is calculated, we obtain the multi-view clustering output by K-means algorithm via the following [45], [46]:

$$\mathcal{L}_{clu} = \min_{U, S} \|\mathbf{Z} - \mathbf{US}\|_F^2, \quad (17)$$

s.t.

$$\mathbf{S} \in \{0, 1\}^{c \times n}, \mathbf{S}^T \mathbf{I} = \mathbf{I},$$

where $\mathbf{U} = [u_1, \dots, u_c] \in \mathbb{R}^{p \times c}$ denotes c optimal cluster centers, $\mathbf{S} \in \{0, 1\}^{c \times n}$, where $S_{q,k}$ indicates whether z_k belongs to the q -th cluster. \mathbf{I} is a vector with all entries as 1. Algorithm 2 summarizes the above whole learning process for DAICS.

IV. EXPERIMENTS

A. Experiment Setting

1) *Datasets*: To demonstrate the performance of the proposed framework, we evaluate DAICS and the compared baseline methods on four multi-view datasets. Tab. I provides a brief description of each dataset. The details are described as follows.

- **Handwritten numerals (HW)** [47]: This dataset is composed of 2,000 data points from 0 to 9 ten digit categories and each class has 200 data points. We adopt 76 Fourier coefficients of the character shapes and 216 profile correlations as two different views.
- **Caltech101-20**: A subset of Caltech101 includes 2386 images of 20 subjects. We follow the setting used in [14] to extract three handcrafted features including SIFT [48] feature, HOG [49] feature and LBP [50] feature as three views.
- **NUS-WIDE-OBJ**: A subset of NUS-WIDE [51] consists of 30,000 images distributed over 31 object categories. In the experiment, we randomly sample 100 images for each category and get 3100 images in total. We use two types of low-level features extracted from these images, including 64-D color histogram, 144-D color correlogram.
- **MNIST**: A widely-used large-scale benchmark data-set consisting of handwritten digit (0~9) images includes

70,000 samples with 28×28 pixels. We adopt the setting used in [52], the first view is the original images, and the other is given by images only highlighting the digit edge.

2) *Evaluation Metrics*: The clustering performance is measured by using three standard evaluation matrices, i.e., Accuracy (**ACC**), Normalized Mutual Information (**NMI**), and **Purity**. For all metrics, the higher value indicates the better performance. More details could be found in [53].

3) *Comparison methods*: To exhibit the superiority of DAICS, we adopt spectral clustering [32] (following [13], [10], we test the spectral clustering with 1 and 2 views, denoted as $\text{SC}_{v=1}$ and $\text{SC}_{v=2}$) and the state-of-the-art deep clustering algorithms as baseline models, including recent deep multi-view clustering methods: Deep Canonical Correlation Analysis (DCCA) [9], Multi-view clustering via Deep Matrix Factorization (MvDMF) [14], Deep Adversarial Multi-view Clustering network (DAMC) [13], End-to-End Adversarial-Attention network for Multi-Modal Clustering (EAMC) [16], Multi-view Spectral Clustering Network (MvSCN) [10]. To validate our merits, we also test typical single-view deep clustering methods: latent space Clustering in Generative Adversarial Networks (ClusterGAN₁) [34], Generative Adversarial Clustering Network (ClusterGAN₂) [19].

4) *Implementation Details*: All the experiments are implemented by using the public toolbox of PyTorch on a standard Ubuntu-16.04 OS with NVIDIA 1080Ti GPUs and 64 GB memory size. We adopt the **Adam** optimizer as our optimization method with its parameters $\beta_1 = 0.5$, $\beta_2 = 0.99$ and learning rate to be $1e-4$. Instead of manually setting $\lambda(t)$, we choose it based on the loss values of samples such that we select only 5% of all samples as input samples to initialize training process, and then decrease $\lambda(t)$ to include all samples at 4/5 of the maximum epoch.

B. Experimental Results

1) *Compared with State of the Arts*: We compare DAICS with the baseline methods. Tab. II shows the clustering results of DAICS and other methods on three datasets. It is obvious that the clustering results of deep multi-view clustering methods significantly outperform the single-view clustering methods. Specifically, our DAICS achieves 97.4% accuracy on HW dataset, which is the best performance. In addition, DAICS also outperforms other deep methods with a clear improvement on both Caltech101-20 and NUS-WIDE-OBJ datasets. Fig. 4 shows the results from the Nemenyi test described when the analysis is performed per dataset. Overall, it is observed that the average rank of our proposed DAICS method is higher than those of the others, and the results perform statistically significant. We attribute this success to adversarial inconsistent samples, cognitive sampling and golden section among multiple views.

2) *Clustering on Large-scale Dataset*: To test the efficiency of DAICS on large-scale dataset, we compare DAICS with three deep models (DCCA, DAMC and EAMC) on MNIST dataset. It is worth noting that, DAICS is efficient due to the cognitive sampling strategy for multi-view clustering. As shown in Tab. III, our proposed method consistently outperforms the other methods in terms of ACC, MNI and Purity,

TABLE I
DATASET DESCRIPTIONS.

Dataset	#image	#view	#class
HW	2,000	2	10
Caltech101-20	2,386	3	20
NUS-WIDE-OBJ	3,100	2	31
MNIST	70,000	2	10

TABLE II
CLUSTERING PERFORMANCE OF OUR PROPOSED DAICS AND BASELINE METHODS OVER HW, CALTECH101-20 AND NUS-WIDE-OBJ DATASETS. RESULTS IN BOLD FACE ARE THE BEST FOR CORRESPONDING METRICS.

Method	HW			Caltech101-20			NUS-WIDE-OBJ		
	ACC \uparrow	NMI \uparrow	Purity \uparrow	ACC \uparrow	NMI \uparrow	Purity \uparrow	ACC \uparrow	NMI \uparrow	Purity \uparrow
SC _{v=1} [32]	0.693	0.674	0.708	0.319	0.447	0.317	0.153	0.155	0.152
SC _{v=2} [32]	0.658	0.651	0.672	0.313	0.416	0.310	0.149	0.141	0.145
ClusterGAN ₁ [34]	0.842	0.829	0.855	0.346	0.445	0.342	0.191	0.184	0.187
ClusterGAN ₂ [19]	0.856	0.833	0.869	0.378	0.496	0.376	0.183	0.188	0.179
DCCA [9]	0.860	0.842	0.877	0.428	0.620	0.426	0.205	0.196	0.203
MvDMF [14]	0.843	0.827	0.854	0.362	0.487	0.360	0.185	0.177	0.182
DAMC [13]	0.954	0.920	0.961	0.534	0.661	0.531	0.243	0.235	0.241
EAMC [16]	0.946	0.925	0.958	0.557	0.674	0.553	0.255	0.238	0.252
MvSCN [10]	0.965	0.957	0.972	0.578	0.690	0.574	0.226	0.221	0.223
DAICS (ours)	0.974	0.951	0.983	0.605	0.728	0.603	0.278	0.265	0.263

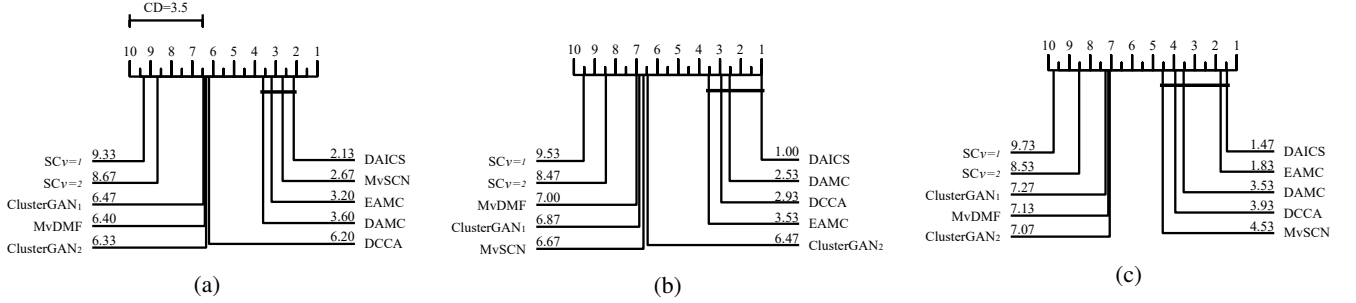


Fig. 4: Comparisons of our proposed DAICS against baseline methods using the Nemenyi test on 15 folds of per dataset ((a) HW, (b) Caltech101-20, (c) NUS-WIDE-OBJ). The methods that are not significantly different at 0.05 level are connected.

TABLE III
CLUSTERING RESULTS ON LARGE-SCALE MNIST DATASET. RESULTS IN BOLD FACE ARE THE BEST FOR CORRESPONDING METRICS.

Method	ACC \uparrow	NMI \uparrow	Purity \uparrow
DCCA [9]	0.472	0.437	0.496
DAMC [13]	0.647	0.598	0.653
EAMC [16]	0.665	0.614	0.649
DAICS (ours)	0.698	0.651	0.693

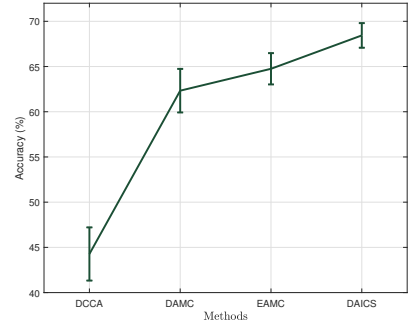


Fig. 5: The mean and standard deviation of the accuracy of DAICS and baseline methods on MNIST dataset.

which validates the superiority of our DAICS on the large-scale dataset.

In order to compare the results more fairly, we repeated the experiment of our proposed DAICS and baseline methods on MNIST dataset for 15 times. The mean and standard deviation of the accuracy of them are shown in Fig. 5 and our proposed DAICS outperforms obviously the baseline methods. To further demonstrate the above fact, we present the visualized results of all these methods on 2500 samples randomly selected from MNIST via the t-SNE. As it is widely known that the visualized results of the t-SNE are more uniform than

the UMAP. Therefore, we only adopt the t-SNE to achieve the visualized results as shown in Fig. 6. It can be easily seen that DAICS offers a more clear and compact cluster structure than other deep models.

3) *Ablation Study*: To further validate the effectiveness of each component for DAICS, extensive ablation studies are performed, including the adversarial inconsistent samples (AIS), the cognitive sampling (CS), and the golden section

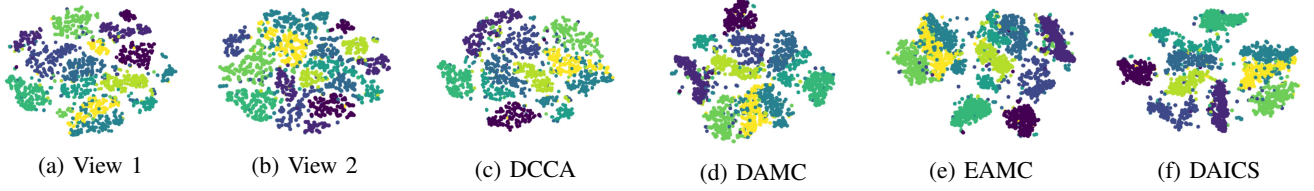


Fig. 6: Visualization of deep multi-view clustering results of four methods ((c) DCCA; (d) DAMC; (e) EAMC; (f) Our proposed DAICS.) via the t-SNE on MNIST dataset with two views: (a) Original features as the first view; (b) Edge features as the second view. We observe that DAICS offers a more clear and compact cluster structure than other methods.

(GS). For brevity, $\text{DAICS}_{\text{NONE}}$ denotes DAICS without the above three components. DAICS_{CS} denotes DAICS with the CS only, since there is no the AIS, we adopt the input samples (from easy to difficult) of the training network with the view that achieves the best performance. $\text{DAICS}_{\text{CS}+\text{GS}}$ makes up the GS to DAICS_{CS} . $\text{DAICS}_{\text{AIS}+\text{CS}}$ denotes DAICS without the GS. Tab. IV. Similarly, we repeated the experiment of our proposed DAICS and different variants on HW dataset for 15 times. Fig. 7 show the mean and standard deviation of the results of the above models on HW dataset. All of the components are effective, due to the following observations:

TABLE IV

ABLATION STUDY ON HW DATASET. RESULTS IN BOLD FACE ARE THE BEST FOR CORRESPONDING METRICS.

Model	ACC \uparrow	NMI \uparrow	Purity \uparrow
$\text{DAICS}_{\text{NONE}}$	0.908	0.892	0.915
DAICS_{CS}	0.926	0.915	0.934
$\text{DAICS}_{\text{CS}+\text{GS}}$	0.927	0.912	0.937
$\text{DAICS}_{\text{AIS}+\text{CS}}$	0.971	0.946	0.976
DAICS	0.974	0.951	0.983

- Upon the results of $\text{DAICS}_{\text{NONE}}$, DAICS_{CS} and $\text{DAICS}_{\text{AIS}+\text{CS}}$, it can be easily seen that the AIS and CS are key components that can avoid getting stuck in non-ideal local minima for the better clustering results.
- Despite the improvement of the GS on clustering results is not obvious from $\text{DAICS}_{\text{AIS}+\text{CS}}$ and DAICS, it can be observed that the GS significantly improves the network

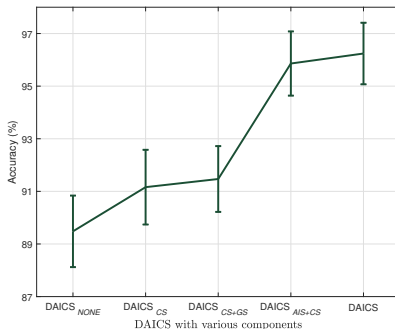


Fig. 7: The mean and standard deviation of the accuracy of DAICS with various components on HW dataset.

efficiency as per Fig. 8.

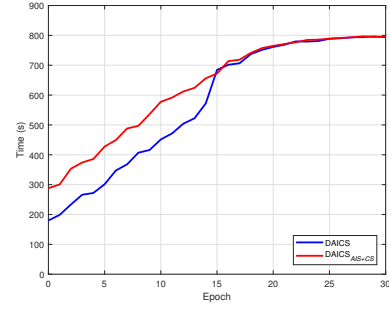


Fig. 8: The effect of the GS on efficiency of DAICS over varied training epochs on HW dataset.

4) *Parameters Analysis:* We conduct parameter analysis of DAICS on HW dataset, including m, ℓ, α and β for our essential AIS module on multi-view clustering. Specifically, the feature similarity loss \mathcal{L}_{sim} and the binary classification loss \mathcal{L}_{adv} are influenced by the margin m and the factor ℓ , respectively. As shown in Fig. 9(a), when $m \in [0.01, 0.1]$, our DAICS can obtain the better clustering performance. Meanwhile, $\ell = 0.5$ is more suitable for DAICS as demonstrated in Fig. 9(b). Besides, the adjustable factors α and β can control

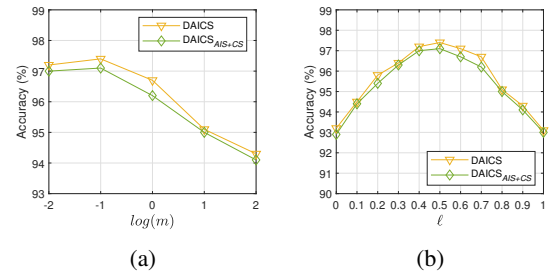


Fig. 9: Clustering performance of $\text{DAICS}_{\text{AIS}+\text{CS}}$ and DAICS with varied values for parameters: (a) The margin m ; (b) The factor ℓ on HW dataset.

the optimization process with an adversarial minimax game of the AIS module. When $\alpha = 0.3$ and $\beta = 0.5$, it can be seen that the best clustering result is obtained about ACC and NMI as shown in Fig. 10(a) and Fig. 10(b).

V. CONCLUSION

In this paper, we propose a novel Deep Adversarial Inconsistent Cognitive Sampling (DAICS) method for multi-view

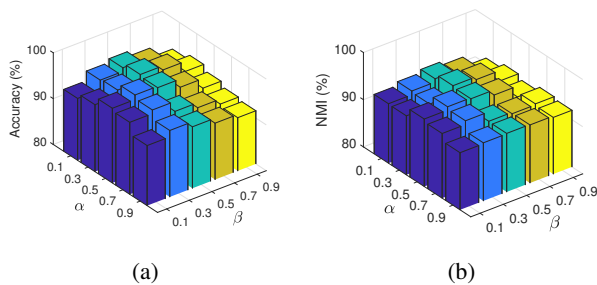


Fig. 10: The effect of the parameters α and β on clustering performance against HW dataset. (a) and (b) are the clustering results in terms of ACC and NMI.

progressive subspace clustering. DAICS consists of the AIS module, the CS strategy and multi-view progressive clustering network with the GS mechanism. The AIS module exploits an adversarial minimax game of the binary classification loss and the feature similarity loss for sample consistency. The CS strategy gradually selects the input samples from easy to difficult for multi-view clustering network training. Moreover, the GS mechanism is developed for efficiency. Experimental results demonstrate that DAICS outperforms the state-of-the-arts over real-world datasets.

REFERENCES

- [1] P. Zhou, Y. Hou, and J. Feng, "Deep adversarial subspace clustering," in *Proceedings of the Conference on Computer Vision and Pattern Recognition*, pp. 1596–1604, 2018.
- [2] X. Yang, C. Deng, F. Zheng, J. Yan, and W. Liu, "Deep spectral clustering using dual autoencoder network," in *Proceedings of the Conference on Computer Vision and Pattern Recognition*, pp. 4066–4075, 2019.
- [3] M. Caron, P. Bojanowski, A. Joulin, and M. Douze, "Deep clustering for unsupervised learning of visual features," in *Proceedings of the European Conference on Computer Vision*, pp. 132–149, 2018.
- [4] Y. Jiang, Z. Yang, Q. Xu, X. Cao, and Q. Huang, "When to learn what: Deep cognitive subspace clustering," in *Proceedings of the ACM International Conference on Multimedia*, pp. 718–726, 2018.
- [5] U. Shaham, K. Stanton, H. Li, R. Basri, B. Nadler, and Y. Kluger, "SpectralNet: Spectral clustering using deep neural networks," in *International Conference on Learning Representations*, 2018.
- [6] P. Ji, T. Zhang, H. Li, M. Salzmann, and I. Reid, "Deep subspace clustering networks," in *Advances in Neural Information Processing Systems*, pp. 24–33, 2017.
- [7] T. Zhang, P. Ji, M. Harandi, W. Huang, and H. Li, "Neural collaborative subspace clustering," in *International Conference on Machine Learning*, pp. 7384–7393, 2019.
- [8] J. Zhang, C.-G. Li, C. You, X. Qi, H. Zhang, J. Guo, and Z. Lin, "Self-supervised convolutional subspace clustering network," in *Proceedings of the Conference on Computer Vision and Pattern Recognition*, pp. 5473–5482, 2019.
- [9] G. Andrew, R. Arora, J. Bilmes, and K. Livescu, "Deep canonical correlation analysis," in *International Conference on Machine Learning*, pp. 1247–1255, 2013.
- [10] Z. Huang, J. T. Zhou, X. Peng, C. Zhang, H. Zhu, and J. Lv, "Multi-view spectral clustering network," in *Proceedings of the International Joint Conference on Artificial Intelligence*, pp. 2563–2569, 2019.
- [11] R. Li, C. Zhang, H. Fu, X. Peng, T. Zhou, and Q. Hu, "Reciprocal multi-layer subspace learning for multi-view clustering," in *Proceedings of the International Conference on Computer Vision*, pp. 8172–8180, 2019.
- [12] D. Hu, F. Nie, and X. Li, "Deep multimodal clustering for unsupervised audiovisual learning," in *Proceedings of the Conference on Computer Vision and Pattern Recognition*, pp. 9248–9257, 2019.
- [13] Z. Li, Q. Wang, Z. Tao, Q. Gao, and Z. Yang, "Deep adversarial multi-view clustering network," in *Proceedings of the International Joint Conference on Artificial Intelligence*, pp. 2952–2958, 2019.
- [14] H. Zhao, Z. Ding, and Y. Fu, "Multi-view clustering via deep matrix factorization," in *Proceedings of the AAAI Conference on Artificial Intelligence*, pp. 2921–2927, 2017.
- [15] Y. Jiang, Q. Xu, Z. Yang, X. Cao, and Q. Huang, "DM2C: Deep mixed-modal clustering," in *Advances in Neural Information Processing Systems*, pp. 5888–5892, 2019.
- [16] R. Zhou and Y. Shen, "End-to-end adversarial-attention network for multi-modal clustering," in *Proceedings of the Conference on Computer Vision and Pattern Recognition*, pp. 14619–14628, 2020.
- [17] R. Hadsell, S. Chopra, and Y. LeCun, "Dimensionality reduction by learning an invariant mapping," in *Proceedings of the Conference on Computer Vision and Pattern Recognition*, pp. 1735–1742, 2006.
- [18] I. Goodfellow, J. Pouget-Abadie, M. Mirza, B. Xu, D. Warde-Farley, S. Ozair, A. Courville, and Y. Bengio, "Generative adversarial nets," in *Advances in Neural Information Processing Systems*, pp. 2672–2680, 2014.
- [19] K. Ghasedi, X. Wang, C. Deng, and H. Huang, "Balanced self-paced learning for generative adversarial clustering network," in *Proceedings of the Conference on Computer Vision and Pattern Recognition*, pp. 4391–4400, 2019.
- [20] C.-G. Li, C. You, and R. Vidal, "On geometric analysis of affine sparse subspace clustering," *IEEE Journal of Selected Topics in Signal Processing*, vol. 12, no. 6, pp. 1520–1533, 2018.
- [21] M. Yamaguchi, G. Irie, T. Kawanishi, and K. Kashino, "Subspace structure-aware spectral clustering for robust subspace clustering," in *Proceedings of the International Conference on Computer Vision*, pp. 9875–9884, 2019.
- [22] C.-G. Li, C. You, and R. Vidal, "Structured sparse subspace clustering: A joint affinity learning and subspace clustering framework," *IEEE Transactions on Image Processing*, vol. 26, no. 6, pp. 2988–3001, 2017.
- [23] E. Elhamifar and R. Vidal, "Sparse subspace clustering: Algorithm, theory, and applications," *IEEE Transactions on Pattern Analysis and Machine Intelligence*, vol. 35, no. 11, pp. 2765–2781, 2013.
- [24] R. Vidal, "Subspace clustering," *IEEE Signal Processing Magazine*, vol. 28, no. 2, pp. 52–68, 2011.
- [25] Y. Wang, X. Lin, L. Wu, W. Zhang, Q. Zhang, and X. Huang, "Robust subspace clustering for multi-view data by exploiting correlation consensus," *IEEE Transactions on Image Processing*, vol. 24, no. 11, pp. 3939–3949, 2015.
- [26] Y. Wang, L. Wu, X. Lin, and J. Gao, "Multiview spectral clustering via structured low-rank matrix factorization," *IEEE Transactions on Neural Networks and Learning Systems*, vol. 29, no. 10, pp. 4833–4843, 2018.
- [27] Y. Wang, Z. Wenjie, L. Wu, X. Lin, M. Fang, and S. Pan, "Iterative views agreement: An iterative low-rank based structured optimization method to multi-view spectral clustering," in *Proceedings of the International Joint Conference on Artificial Intelligence*, pp. 2153–2159, 2016.
- [28] G. Liu, Z. Lin, S. Yan, J. Sun, Y. Yu, and Y. Ma, "Robust recovery of subspace structures by low-rank representation," *IEEE Transactions on Pattern Analysis and Machine Intelligence*, vol. 35, no. 1, pp. 171–184, 2012.
- [29] R. Vidal and P. Favaro, "Low rank subspace clustering," *Pattern Recognition Letters*, vol. 43, pp. 47–61, 2014.
- [30] L. Wu, Y. Wang, and L. Shao, "Cycle-consistent deep generative hashing for cross-modal retrieval," *IEEE Transactions on Image Processing*, vol. 28, no. 4, pp. 1602–1612, 2018.
- [31] Y. Wang, "Survey on deep multi-modal data analytics: Collaboration, rivalry, and fusion," *ACM Transactions on Multimedia Computing, Communications, and Applications*, vol. 17, no. 1, pp. 1–25, 2021.
- [32] A. Y. Ng, M. I. Jordan, and Y. Weiss, "On spectral clustering: Analysis and an algorithm," in *Advances in Neural Information Processing Systems*, pp. 849–856, 2002.
- [33] Y. Jiang, Q. Xu, Z. Yang, X. Cao, and Q. Huang, "Duet robust deep subspace clustering," in *Proceedings of the ACM International Conference on Multimedia*, pp. 1596–1604, 2019.
- [34] S. Mukherjee, H. Asnani, E. Lin, and S. Kannan, "ClusterGAN: Latent space clustering in generative adversarial networks," in *Proceedings of the AAAI Conference on Artificial Intelligence*, pp. 4610–4617, 2019.
- [35] Y. Bengio, J. Louradour, R. Collobert, and J. Weston, "Curriculum learning," in *Proceedings of the International Conference on Machine Learning*, pp. 41–48, 2009.
- [36] M. P. Kumar, B. Packer, and D. Koller, "Self-paced learning for latent variable models," in *Advances in Neural Information Processing Systems*, pp. 1189–1197, 2010.
- [37] L. Jiang, D. Meng, S.-I. Yu, Z. Lan, S. Shan, and A. Hauptmann, "Self-paced learning with diversity," *Advances in Neural Information Processing Systems*, vol. 27, pp. 2078–2086, 2014.

- [38] H. Li, M. Gong, D. Meng, and Q. Miao, "Multi-objective self-paced learning," in *Proceedings of the AAAI Conference on Artificial Intelligence*, pp. 1802–1808, 2016.
- [39] J. Liang, Z. Li, D. Cao, R. He, and J. Wang, "Self-paced cross-modal subspace matching," in *Proceedings of the International ACM SIGIR Conference on Research and Development in Information Retrieval*, pp. 569–578, 2016.
- [40] D. Zhang, D. Meng, C. Li, L. Jiang, Q. Zhao, and J. Han, "A self-paced multiple-instance learning framework for co-saliency detection," in *Proceedings of the IEEE International Conference on Computer Vision*, pp. 594–602, 2015.
- [41] H. Gao and H. Huang, "Self-paced network embedding," in *Proceedings of the ACM SIGKDD International Conference on Knowledge Discovery & Data Mining*, pp. 1406–1415, 2018.
- [42] W. Chen, X. Chen, J. Zhang, and K. Huang, "Beyond triplet loss: A deep quadruplet network for person re-identification," in *Proceedings of the Conference on Computer Vision and Pattern Recognition*, pp. 403–412, 2017.
- [43] Y. Zhong and W. Deng, "Adversarial learning with margin-based triplet embedding regularization," in *Proceedings of the International Conference on Computer Vision*, pp. 6549–6558, 2019.
- [44] C. Xu, Z. Guan, W. Zhao, H. Wu, Y. Niu, and B. Ling, "Adversarial incomplete multi-view clustering," in *Proceedings of the International Joint Conference on Artificial Intelligence*, pp. 3933–3939, 2019.
- [45] F. Nie, C.-L. Wang, and X. Li, "K-multiple-means: A multiple-means clustering method with specified k clusters," in *Proceedings of the ACM SIGKDD International Conference on Knowledge Discovery & Data Mining*, pp. 959–967, 2019.
- [46] S. Xia, D. Peng, D. Meng, C. Zhang, G. Wang, E. Giem, W. Wei, and Z. Chen, "A fast adaptive k-means with no bounds," *IEEE Transactions on Pattern Analysis and Machine Intelligence*, 2020.
- [47] A. Asuncion and D. Newman, "UCI machine learning repository," <http://archive.ics.uci.edu/ml/>, 2007.
- [48] D. G. Lowe, "Distinctive image features from scale-invariant keypoints," *International Journal of Computer Vision*, vol. 60, no. 2, pp. 91–110, 2004.
- [49] N. Dalal and B. Triggs, "Histograms of oriented gradients for human detection," in *Proceedings of the Conference on Computer Vision and Pattern Recognition*, pp. 886–893, 2005.
- [50] T. Ojala, M. Pietikainen, and T. Maenpaa, "Multiresolution gray-scale and rotation invariant texture classification with local binary patterns," *IEEE Transactions on Pattern Analysis and Machine Intelligence*, vol. 24, no. 7, pp. 971–987, 2002.
- [51] T.-S. Chua, J. Tang, R. Hong, H. Li, Z. Luo, and Y. Zheng, "NUS-WIDE: A real-world web image database from national university of singapore," in *Proceedings of the ACM International Conference on Image and Video Retrieval*, pp. 1–9, 2009.
- [52] C. Shang, A. Palmer, J. Sun, K.-S. Chen, J. Lu, and J. Bi, "VIGAN: Missing view imputation with generative adversarial networks," in *Proceedings of the IEEE International Conference on Big Data*, pp. 766–775, 2017.
- [53] A. Kumar, P. Rai, and H. Daume, "Co-regularized multi-view spectral clustering," in *Advances in Neural Information Processing Systems*, pp. 1413–1421, 2011.